Check for updates

Global Biogeochemical Cycles

RESEARCH ARTICLE
10.1029/2022GB007541

Increased Biogenic Calcification and Burial Under Elevated pCO_2 During the Miocene: A Model-Data Comparison

Weimin Si[1], Timothy Herbert[1], Mengxi Wu[2], and Yair Rosenthal[3]

[1]Department of Earth, Environmental and Planetary Sciences, Brown University, Providence, RI, USA, [2]Joint Institute for Regional Earth System Science and Engineering, University of California Los Angeles, Los Angeles, CA, USA, [3]Department of Marine and Coastal Sciences, Rutgers University, New Brunswick, NJ, USA

Key Points:

- Pelagic carbonate production during the warm Middle Miocene was approximately doubled relative to present-day values
- Net pelagic carbonate burial of the Middle Miocene was likely ~30%–45% higher than modern values
- The decreases in $[Ca^{2+}]_{sw}$ and carbonate production toward the present kept Neogene dissolved inorganic carbon and total alkalinity nearly constant despite a global pCO_2 decrease

Supporting Information:

Supporting Information may be found in the online version of this article.

Correspondence to:

W. Si,
weimin_si@brown.edu

Citation:

Si, W., Herbert, T., Wu, M., & Rosenthal, Y. (2023). Increased biogenic calcification and burial under elevated pCO_2 during the Miocene: A model-data comparison. *Global Biogeochemical Cycles*, *37*, e2022GB007541. https://doi.org/10.1029/2022GB007541

Received 2 AUG 2022
Accepted 14 MAY 2023

© 2023. The Authors.
This is an open access article under the terms of the Creative Commons Attribution License, which permits use, distribution and reproduction in any medium, provided the original work is properly cited.

Abstract Ocean acidification due to anthropogenic CO_2 emission reduces ocean pH and carbonate saturation, with the projection that marine calcifiers and associated ecosystems will be negatively affected in the future. On longer time scale, however, recent studies of deep-sea carbonate sediments suggest significantly increased carbonate production and burial in the open ocean during the warm Middle Miocene. Here, we present new model simulations in comparison to published Miocene carbonate accumulation rates to show that global biogenic carbonate production in the pelagic environment was approximately doubled relative to present-day values when elevated atmospheric pCO_2 led to substantial global warming ~13–15 million years ago. Our analysis also finds that although high carbonate production was associated with high dissolution in the deep-sea, net pelagic carbonate burial was approximately 30%–45% higher than modern. At the steady state of the long-term carbon cycle, this requires an equivalent increase in riverine carbonate alkalinity influx during the Middle Miocene, attributable to enhanced chemical weathering under a warmer climate. Elevated biogenic carbonate production resulted in a Miocene ocean that had carbon (dissolved inorganic carbon) and alkalinity (total alkalinity) inventories similar to modern values but was poorly buffered and less saturated in both the surface and the deep ocean relative to modern.

1. Introduction

Anthropogenic CO_2 emissions are anticipated to impact marine calcifiers in the near future (Feely et al., 2004) due to increasing ocean temperatures (Bijma et al., 1990; Hoegh-Guldberg et al., 2007; Orr et al., 2005; Reynaud et al., 2003) and decreasing carbonate supersaturation of seawater (Fabry et al., 2008; Hoegh-Guldberg et al., 2007; Kleypas et al., 2005; Raven et al., 2005). In laboratory experiments with lower pH and lower $[CO_3^{2-}]$, decreases in calcification have been widely observed in both multicellular metazoans (Albright et al., 2018; Jokiel et al., 2008) and single-celled eukaryotes, including zooplankton planktonic foraminifera and phytoplankton coccolithophores (Bach et al., 2012; de Nooijer et al., 2009; Lombard et al., 2010; Meyer & Riebesell, 2015; Riebesell et al., 2000).

Coccolithophores and planktonic foraminifera are two major contributors to marine carbon cycles. In the open ocean, these micro-organisms consume ~50–130 Tmol of carbonate alkalinity in the surface ocean each year during shell formation (Berelson et al., 2007; Jin et al., 2006; Lee, 2001) and together contribute to more than 50% of global carbonate production (Milliman, 1993). Upon death, sinking calcareous skeletons facilitate the biological pump by increasing the export of organic carbon to the ocean's interior through ballasting (Ziveri et al., 2007). In the deep sea, the burial of their calcareous remains over millions of years provides one of the ultimate sinks for both carbon and alkalinity of Earth's surficial reservoir (In this study, we focus on the discussion of carbonate alkalinity and assume carbonate alkalinity ≈ TA).

Pelagic carbonate records also offer a unique opportunity to study the effects of past ocean acidification on calcifying species (Hönisch et al., 2012). In contrast to culturing observations, several recent studies suggest that carbonate production seems to have been elevated during past warm climate when pCO_2 was also higher, particularly via an increased contribution of calcifying primary producers (Bolton et al., 2016; Si & Rosenthal, 2019; Suchéras-Marx & Henderiks, 2014). These new observations raise questions regarding the effects of pCO_2 on marine phytoplankton (Bolton & Stoll, 2013) and potential long-term evolutionary adaptations of calcifying species to high pCO_2 (Slater et al., 2022). Equally important, because pelagic carbonate production plays an essential role in modulating seawater carbonate chemistry (Broecker, 2003; Ridgwell & Zeebe, 2005), an accurate

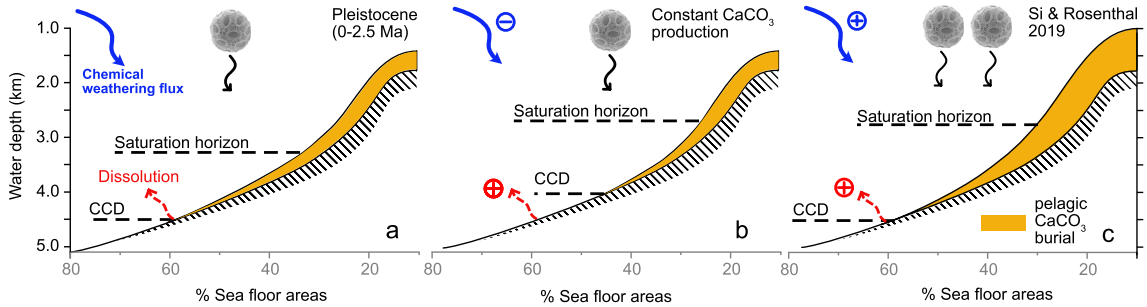

Figure 1. Comparison of different scenarios of the long-term carbon cycling. (a) The Pleistocene is considered as the reference case, with Calcite Compensation Depth (CCD) and saturation horizon located at ~4,500 and ~3,200m in the Pacific, respectively. (b) Assuming constant $CaCO_3$ production rate, a decrease in chemical weathering flux will shoal the CCD and the saturation horizon. (c) Simultaneous increases in $CaCO_3$ production and chemical weathering flux shoal the saturation horizon but maintain the CCD relatively constant. $CaCO_3$ burial rates at shallow water depth are higher in scenario (c) than in (a, b). Note that the *y* axis is exaggerated for the purpose of illustration.

reading of the history of carbonate production and dissolution in the ocean is essential to understand the connection between the global carbon cycle and climatic variations in the past.

2. Late Neogene Paradox of Increased Carbonate Burial in a More Corrosive Ocean

An often-applied approach to studying past changes in marine carbonate cycle is to examine the variation of Calcite Compensation Depth (CCD). The CCD is the depth in the ocean below which there is little to no carbonate burial (a cut-off we use here is <20% $CaCO_3$) and therefore is an indicator of seawater saturation at depth (Figure 1). By assuming that biogenic carbonate production remains approximately constant in the surface ocean (Figures 1a and 1b), a deeper CCD is typically interpreted as less carbonate dissolution due to a more saturated deep ocean. During the Cenozoic (0–66 Ma), the CCD is known to be negatively correlated to the secular variations of pCO_2. Specifically, the long-term cooling from the greenhouse climate of the Eocene (>40 Ma) into the icehouse of the Pleistocene (<3 Ma) is associated with a large decrease in pCO_2 (Hönisch et al., 2012; Rae et al., 2021) as well as the deepening of the Calcite Compensation Depth (CCD) (Pälike et al., 2012; Van Andel, 1975). This co-evolution between pCO_2 and the CCD thus seems to suggest that the deep ocean was unfavorable to carbonate preservation under higher pCO_2, in line with modern observations of ocean acidification on carbonate preservation (Sulpis et al., 2018).

The acid-base equilibria viewpoint is, however, not consistent with the expectation from the mass balance of the marine carbon and alkalinity budgets. The long-term steady state of the carbon cycle and thus Earth's climate is arguably maintained by the silicate weathering feedback, which removes CO_2 degassed from the Earth's interior through chemical weathering on land (Berner & Kothavala, 2001; Berner et al., 1983; Walker et al., 1981). The weathering product is delivered to the ocean as carbonate alkalinity and ultimately preserved in sediments as biogenic carbonate. Therefore, it is expected that higher pCO_2 and warmer climate should enhance chemical weathering (both silicate and carbonate) and $CaCO_3$ burial. In other words, the steady state of the long-term carbon cycle predicts that past global warming with high atmospheric pCO_2 concentration should correspond to a more saturated deep ocean and deeper CCD, not vice versa.

Puzzled by the geological evidence of a shallower CCD (an apparently less saturated ocean) under a warmer climate, Si and Rosenthal (2019) investigated pelagic carbonate burial in the world's oceans over the past 13 Myr (the Middle Miocene to the present). They found that biogenic carbonate production and accumulation in the open ocean were both higher when pCO_2, global temperatures, and deep water corrosivity (we define "corrosive" as more $CaCO_3$ dissolution due to undersaturation) were all much higher than today (Figure 1c, Herbert et al., 2016; Rae et al., 2021; Si & Rosenthal, 2019; Sosdian, Rosenthal, & Toggweiler, 2018).

Higher pelagic carbonate production during the Miocene is also supported by micropaleontologic works based on morphometric measurements of coccolith fossils, which reveals both trends of downsizing in coccolithophorid species (Suchéras-Marx & Henderiks, 2014) and reduced calcification (Bolton et al., 2016) in the last 15 Myr as pCO_2 decreased. The decreases in carbonate production not only occurred in the mid-latitude, where cyclic glaciations can have large impacts on regional climate, but are also seen in the tropics (Si & Rosenthal, 2019), where changes in temperatures and phytoplankton compositions (i.e., coccolithophores vs. diatoms) were small.

19449224, 2023, 6, Downloaded from https://agupubs.onlinelibrary.wiley.com/doi/10.1029/2022GB007541, Wiley Online Library on [26/05/2023]. See the Terms and Conditions (https://onlinelibrary.wiley.com/terms-and-conditions) on Wiley Online Library for rules of use; OA articles are governed by the applicable Creative Commons License

19449224, 2023, 6, Downloaded from https://agupubs.onlinelibrary.wiley.com/doi/10.1029/2022GB007541, Wiley Online Library on [26/05/2023]. See the Terms and Conditions (https://onlinelibrary.wiley.com/terms-and-conditions) on Wiley Online Library for rules of use; OA articles are governed by the applicable Creative Commons License

Si and Rosenthal (2019) proposed that the apparent paradox of more carbonate burial in a more corrosive deep ocean during the Miocene arises from a much larger increase in pelagic carbonate production relative to a smaller increase in continental chemical weathering. Higher chemical weathering fluxes require that the ocean as a whole has more carbonate burial to balance the alkalinity throughput; meanwhile, increased carbonate production allocates more carbonate burial to shallower parts of the ocean and thus requiring a more corrosive deep sea to balance carbonate overproduction in the surface ocean (Figure 1c). A similar scenario has been argued to explain the higher carbonate burial rates in the western equatorial Pacific during interglacial intervals of the mid-and late Pleistocene (Sosdian, Rosenthal, & Toggweiler, 2018).

Si and Rosenthal (2019), however, did not provide any quantitative estimates on the changes in global pelagic carbonate mass accumulation rates—a factor ultimately critical to the mass balance of weathering fluxes. They also did not address how the saturation state of the surface ocean ($\Omega = [Ca^{2+}][CO_3^{2-}]_{sw}/K_{sp}$, where K_{sp} is solubility product constant of calcium carbonate) might have changed in association with changes in pelagic carbonate production. Previous studies have pointed out an important distinction between low pH and low Ω (Hönisch et al., 2012). It is possible that past oceans had lower than present pH but a high Ω in the surface ocean, such as was the case in the Eocene and the Cretaceous (Hönisch et al., 2012). Because it is the saturation state of the surface ocean, rather than the pH, that matters to calcification, it is possible that higher $CaCO_3$ production proposed by Si and Rosenthal (2019) was actually associated with a more saturated surface ocean during the Miocene.

Here, we perform a model-data analysis on mid-Miocene carbonate production and mass accumulation rates. The model we use is the Earth System model of intermediate complexity (cGENIE) (Ridgwell et al., 2021) and the published Miocene carbonate accumulation (MARc) data for comparison are from Si and Rosenthal (2019). Our goals are two-fold: (a) quantitatively estimate Miocene global pelagic carbonate production and continental weathering flux by comparing model results with CCD and MARc reconstructions from various water depths of the ocean and (b) investigate the implications of elevated carbonate production on seawater carbonate chemistry, focusing on the ocean's saturation state (Ω), dissolved inorganic carbon (DIC), TA inventories and buffering capacity.

3. The Steady State of Ocean's Carbonate Chemistry

Seawater carbonate chemistry has six variables (CO_2, H_2CO_3, HCO_3^-, CO_3^{2-}, H^+ and OH^-) and four equilibrium constants, leaving two degrees of freedom to fully constrain the system. From the aspect of the long-term carbon cycle, these two degrees of freedom are ultimately controlled by two "external" processes, CO_2 degassing from the Earth's interior and (continental) silicate weathering. Together they impose direct controls on atmospheric pCO_2 and seawater carbonate ion concentrations ($[CO_3^{2-}]_{sw}$) through the chemical weathering feedback.

On short timescales, such as glacial-interglacial transitions, changes in ocean circulation control the partitioning of carbon between the deep ocean and the atmosphere and therefore affect atmospheric pCO_2 (Toggweiler & Sarmiento, 1985). On million-year timescales, the primary control on pCO_2 is the need for the mass balance (Berner & Caldeira, 1997; Broecker & Sanyal, 1998). Atmospheric pCO_2 will respond to changes in CO_2 degassing rates (Berner et al., 1983; Walker et al., 1981) and/or changes in silicate weatherability (Kump & Arthur, 1997; Raymo et al., 1988) so that Earth's greenhouse effect adjusts the silicate weathering fluxes in an attempt to match the total CO_2 coming out from the Earth's interior. In this regard, pCO_2 acts as a "policeman" to regulate the carbon "traffic" so that the system can remain close to the steady state. The ocean will come in equilibrium with the atmosphere pCO_2 on the tectonic timescale, not vice versa.

The pCO_2 level that is needed to guarantee the above-mentioned mass balance is referred to as the steady-state pCO_2 hereafter. It is important to note that steady-state pCO_2 does not mean pCO_2 remains invariant over time. Instead, it refers to the long-term mean at mass balance. For instance, in the Late Pleistocene, pCO_2 varied between 180–280 p.p.m.v. in association with orbitally paced glacial-interglacial cycles; the long-term trend, however, is no more than 22 p.p.m.v. over the past 600 kyr and the maximum imbalance between the supply and uptake of CO_2 is estimated within 1%–2% (Zeebe & Caldeira, 2008).

Given the steady state pCO_2, chemical weathering on land consumes CO_2 at a rate equal to the volcanic CO_2 outgassing fluxes and delivers weathered products to the ocean mainly in the form of carbonate alkalinity, driving changes in $[CO_3^{2-}]_{sw}$ so that carbonate burial rates in the deep-sea can balance riverine alkalinity inputs.

19449224, 2023, 6, Downloaded from https://agupubs.onlinelibrary.wiley.com/doi/10.1029/2022GB007541, Wiley Online Library on [26/05/2023]. See the Terms and Conditions (https://onlinelibrary.wiley.com/terms-and-conditions) on Wiley Online Library for rules of use; OA articles are governed by the applicable Creative Commons License

Table 1
Miocene Scenarios Examined in This Study, Including Two pCO_2 (600 and 1,120 p.p.m.v., We Use "+" to Indicate 1,120 p.p.m.v. Scenario), Two Carbonate Production (1x and 2x) and Three Weathering Flux Levels (1x, 1.3x, and 1.45x)

Miocene 600 p.p.m.v. (1,120 p.p.m.v.)		
	1.0x carbonate production	2.0x carbonate production
1.0x weathering flux	Ma (Ma+)	Mc (Mc+)
1.3x weathering flux	Mb (Mb+)	Md (Md+)
1.45x weathering flux	-----	Me (Me+)
Control experiment		
Pre-industrial (288 p.p.m.v.)		
1.0x weathering fluxes and 1.0x carbonate production		

Changes in carbonate production rates in the surface ocean can also modulate $[CO_3^{2-}]_{sw}$ by changing the depth distribution of carbonate accumulation. Higher pelagic carbonate production and/or shelf carbonate accumulation, for instance, will deposit more carbonate to relatively shallow depths (i.e., above the carbonate lysocline), driving a decrease in $[CO_3^{2-}]_{sw}$ so that more dissolution can occur at deeper depths to keep the ocean's alkalinity budget in balance (Broecker, 2003; Si & Rosenthal, 2019).

In short, the ocean's carbonate chemistry at steady state is a function of steady-state pCO_2 and weathering alkalinity inputs. Changes in pelagic carbonate production also play a role due to its capability to shift the locus of carbonate burial and therefore modify $[CO_3^{2-}]_{sw}$. In this work, we perform a set of carbon cycle model simulations using a range of atmospheric pCO_2 (600 and 1,120 p.p.m.v.), weathering alkalinity inputs (1x, 1.3x, and 1.45x of modern), and pelagic carbonate production rates (1x and 2x of modern) (Table 1) are tested, followed by evaluation based on reconstructed CCD, MARc, and seawater chemistry from published studies (Pälike et al., 2012; Si & Rosenthal, 2019; Sosdian, Greenop, et al., 2018; Zeebe & Tyrrell, 2019). MARc above the carbonate saturation horizon will provide first-order estimates on the carbonate production rate in the surface ocean; the changes in MARc over water depth then put constraints on the relative contribution of production versus dissolution. Combined with reconstructions of the CCD, we will be able to estimate net carbonate burial over the water column and thus infer the alkalinity weathering input.

4. Modeling Overproduction of Pelagic Carbonate

In the modern ocean, global rivers deliver ~33 Tmol of alkalinity to the ocean per year (Cai et al., 2008). Pelagic calcifiers, however, consume ~50–130 Tmol of alkalinity through calcification (Berelson et al., 2007; Jin et al., 2006; Lee, 2001; Milliman, 1993). Because of this overproduction, the deep ocean is necessarily undersaturated in order to remove excessive biogenic carbonate through dissolution (Broecker, 1971; Ridgwell & Zeebe, 2005; Zeebe & Westbroek, 2003). As Si and Rosenthal (2019) pointed out, the key to understanding the late Neogene carbonate paradox is the ecologically driven change in the overproduction of pelagic carbonate relative to the changes in weathering alkalinity flux.

Box models are often used for long-term carbon cycle analysis. In simplified box models, carbonate production, however, is often treated as a function of ocean saturation in the past relative to the modern (Boudreau et al., 2019; Krissansen-Totton & Catling, 2017; Rugenstein et al., 2019). This simplification consists of two crucial assumptions. First, carbonate production is proportional to carbonate saturation Ω. Second, carbonate production is always equal to carbonate burial and weathering alkalinity input because the dissolution of carbonate produced in excess of mass balance is not explicitly considered in these types of box models. Given these simplifications, a deepening of the CCD throughout the Neogene, which indicates increasing saturation over time, leads these models to infer that deep-sea carbonate burial has increased over time, apparently implying less than present-day chemical weathering fluxes during the Miocene.

Because the magnitude of carbonate overproduction may have changed independently of (or even opposed to) the saturation state of the ocean (Si & Rosenthal, 2019), models that explicitly parameterize both the *overproduction* of biogenic carbonates in the surface ocean (relative to weathering alkalinity input) and the dissolution in the deep sea (Ridgwell & Hargreaves, 2007; Zeebe, 2012) are therefore necessary to study the long-term carbon cycle. Here we use cGENIE because it has a 3D ocean (36 × 36 equal area grid with 16 non-equally spaced vertical levels in this study) that can simulate spatial variations in carbonate production and preservation that box models cannot (Ridgwell et al., 2021). Major carbonate provinces such as the equatorial Pacific owe their existence to high primary productivity in association with active upwelling and high preservation due to the topographic high of mid-ocean ridges beneath the upwelling zone. This coupling between ocean circulation, productivity, and seafloor hypsometry can be reasonably represented in cGENIE.

As an open-sourced model, cGENIE ("muffin" release) also allows for developing new experiments based on published studies. Here we use the recent Miocene simulations developed by Crichton et al. (2021) as the basic

19449224, 2023, 6, Downloaded from https://agupubs.onlinelibrary.wiley.com/doi/10.1029/2022GB007541, Wiley Online Library on [26/05/2023]. See the Terms and Conditions (https://onlinelibrary.wiley.com/terms-and-conditions) on Wiley Online Library for rules of use; OA articles are governed by the applicable Creative Commons License

configuration of our work. This particular implementation of the cGENIE model comprises mid-Miocene continental and surface boundary conditions derived from fully coupled GCM experiments. Salinity flux adjustment is then used to find the circulation pattern that best reproduces the Miocene carbon isotope records (please refer to Section 2.2 of Crichton et al. (2021) for details of model configurations). In this work, we keep all parameters the same as in the original study except for modifications on pCO_2 levels, global pelagic carbonate production rates, and weathering alkalinity flux. A combination of ten mid-Miocene scenarios, with one additional pre-industrial run as a control experiment, are examined (Table 1). Details on weathering flux, carbonate production, and burial rates are provided in Table S1 in Supporting Information S1.

Modifications on pCO_2 forcing and weathering alkalinity flux follow the standard practice in cGENIE modeling (Ridgwell et al., 2021). In order to force changes in pelagic carbonate production, we manipulate PIC:POC ratio in each scenario so that organic productivity can remain the same as Crichton et al. (2021). The distribution of $\delta^{13}C$ of benthic foraminifera is a function of the organic biological pump and ocean circulation. By holding organic productivity the same as the original model and modifying the PIC:POC ratio only, our new simulations do not change simulated $\delta^{13}C$ patterns in the original model, which has been shown to be largely consistent with the $\delta^{13}C$ distribution of benthic foraminifera (Crichton et al., 2021). All configuration files are available in Supporting Information S1. For each simulation, we perform a spin-up run for 500 kyr following Ridgwell and Hargreaves (2007) and then run with no acceleration for 80 kyr. Only the last 10 kyr are saved. The steady-state carbonate burial flux is available in Table S1 in Supporting Information S1. All simulations are completed using the Oscar cluster at the Center for Computation and Visualization, Brown University.

5. Results

Figure 2 shows MARc and $CaCO_3$(%) from the Pacific Ocean (65°N–50°S, 125°E–80°W) in 11 cGENIE simulations (gray color) in comparison to downcore MARc from Si and Rosenthal (2019) (Blue circles: Pleistocene 0–2.7 Ma; Red circles: Middle Miocene 11.5–13.5 Ma). We choose the Pacific Ocean because its size, and therefore its carbonate chemistry, is most representative of the global ocean. The red vertical line indicates 20% carbonate percentage, which is often used to indicate the CCD. Black arrows indicate the average depth of Pleistocene CCD (Farrell & Prell, 1991), which is used here to approximate the steady state CCD of the last 2 Myr.

In theory, a strict model-data comparison should retrieve model results from where proxy data are available so that model and data discrepancies can be directly calculated for statistical evaluation. However, this is not possible because Si and Rosenthal (2019) have targeted MARc estimates from closely spaced sites along depth transects (e.g., Ontong Java Plateau) in order to resolve the effects of production versus dissolution, while cGENIE has a relatively low spatial resolution (36 × 36 equal area grid). As a result, we compare the data and modeled MARc as a regional (Pacific) composite in Figure 2.

Scenario "P" (Figure 2, panel 1) represents the pre-industrial experiment with 280 p.p.m.v., carbonate production (1x = 41.6 Tmol/yr) in the range of modern estimate (Berelson et al., 2007; Jin et al., 2006; Lee, 2001; Milliman, 1993), and modern weathering alkalinity flux (1x = 33 Tmol/yr) (Cai et al., 2008). Because we focus on simulating the steady state, we use the average Pleistocene MARc reported by Si and Rosenthal (2019) for comparison. Here, cGENIE produces carbonate burial rates consistent with sediment core records. The model does seem to slightly overestimate $CaCO_3$(%) below 4,000 m and therefore leads to a CCD slightly deeper than the Pleistocene average (black arrows). We also compare vertical profiles of seawater carbonate chemistry in cGENIE versus in GLODAP database (Lauvset et al., 2021) (Figure S1 in Supporting Information S1). There is an overall good agreement between the model and observations.

Scenarios Ma (Ma+) are forced with present-day weathering flux (1x) and carbonate production (1x) but different pCO_2 (Ma = 600 and Ma+ = 1,120 p.p.m.v., respectively). Model results show that when carbonate production and weathering alkalinity remain the same as today, MARc and $CaCO_3$(%) also stay unchanged (Figure 2, panel 2), despite higher than present-day pCO_2. Noticeably, mid-Miocene MARc from downcore measurements are significantly higher than model results, particularly at shallow depths. Also noteworthy is that although the different pCO_2 levels do not affect carbonate burial, they do change seawater carbonate chemistry (DIC, TA, and pH), which will be addressed later (Section 6.2).

Scenarios Mb (Mb+) are forced with present-day carbonate production (1x), 30% higher chemical weathering flux (1.3x), and pCO_2 of 600 and 1,120 p.p.m.v., respectively. Evidently, the increase in the alkalinity input has

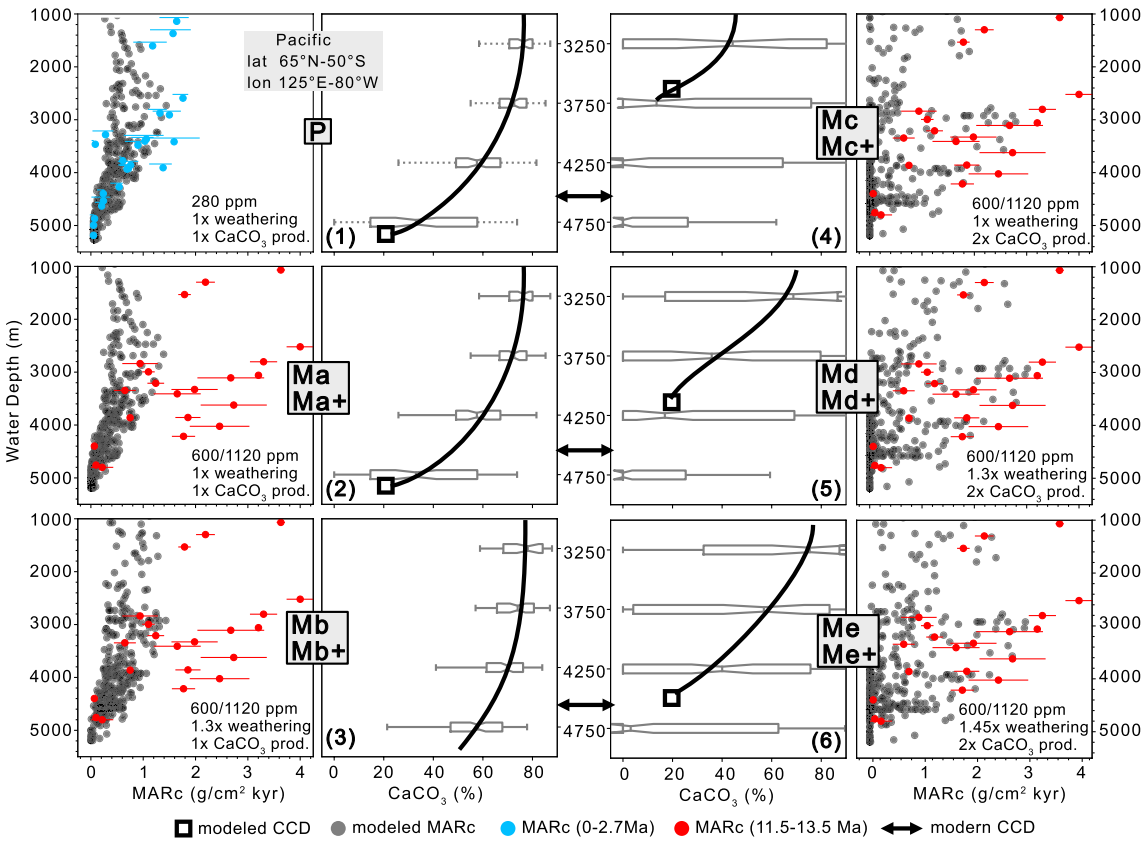

Figure 2. Model-data comparison of Pacific published Miocene carbonate accumulation (MARc) and $CaCO_3$(%). Semi-transparent black circles (MARc) and gray histograms (%$CaCO_3$) are cGENIE model results; Blue and Red circles are MARc in the Pleistocene (0–2.7 Ma) and the Middle Miocene (11.5–13.5 Ma), respectively. Black arrows indicate average Pleistocene Calcite Compensation Depth (Farrell & Prell, 1991; Pälike et al., 2012). P: pre-industrial control run; Ma: 1.0x $CaCO_3$ production, 1.0x weathering flux; Mb: 1.0x production, 1.3x weathering flux; Mc: 2.0x production, 1.0x weathering flux; Md: 2.0x production, 1.3x weathering flux; Me: 2.0x production, 1.45x weathering flux; Simulations Ma-Me have pCO_2 = 600 p.p.m.v., symbol + indicates additional experiments with pCO_2 elevated to 1,120 p.p.m.v.

little effect on modeled MARc at shallow water depth. Instead, it deepens the CCD significantly in the model (Figure 2, panel 3), which is in contradiction to the observation of a slightly shallower or stable CCD during the Miocene (Pälike et al., 2012; Van Andel, 1975). It is important to note that the CCD is highly variable through time and space. Change in local productivity, ocean circulations and dynamic topography can all complicate the reconstruction of regional CCD (Campbell et al., 2018; Dutkiewicz & Müller, 2021; Lyle, 2003). However, a large model-implied deepening of the CCD to ~6,000 m (not shown) with 50% $CaCO_3$ at 5,000 m (Figure 2, panel 3) strongly suggests that scenario Mb (Mb+) increases data-model discrepancy rather than narrows it.

Scenarios Mc (Mc+) are forced with present-day weathering alkalinity fluxes (1x), doubled carbonate production (2x) in the surface ocean and pCO_2 of 600 and 1,120 p.p.m.v. respectively. As a result of higher carbonate productivity, modeled MARc begins to match the observations in the shallow part of the ocean. However, holding weathering alkalinity input at modern value leads to large shoaling of the CCD to above 3,725 m (Figure 2, panel 4). This, again, is not supported by the CCD reconstructions and the fact that carbonate-rich Miocene sediments are available from the deep Pacific at ~3,700 m water depth (e.g., ODP Site 804 and U1307, U1308) (Pälike et al., 2012; Si & Rosenthal, 2019).

In scenarios Md (Md+) and Me (Me+), both carbonate production (2x) and weathering alkalinity flux (1.3x in Md/Md+ and 1.45x in Me/Me+) are higher than modern values. This results in a simultaneously improved agreement between modeled MARc, $CaCO_3$(%) and paleo-records. The CCD is ~4,250 m in Md (Md+) scenario (Figure 2, panel 5) and ~4,500–4,600 m in scenarios Me (Me+) (Figure 2, panel 6). Both are within the uncertainties of paleo-CCD estimates, which suggests that the Miocene CCD was at most ~500 m shallower than the Pleistocene average (~4,800 m) (Pälike et al., 2012; Van Andel, 1975).

19449224, 2023, 6, Downloaded from https://agupubs.onlinelibrary.wiley.com/doi/10.1029/2022GB007541, Wiley Online Library on [26/05/2023]. See the Terms and Conditions (https://onlinelibrary.wiley.com/terms-and-conditions) on Wiley Online Library for rules of use; OA articles are governed by the applicable Creative Commons License

19449224, 2023, 6, Downloaded from https://agupubs.onlinelibrary.wiley.com/doi/10.1029/2022GB007541, Wiley Online Library on [26/05/2023]. See the Terms and Conditions (https://onlinelibrary.wiley.com/terms-and-conditions) on Wiley Online Library for rules of use; OA articles are governed by the applicable Creative Commons License

6. Discussion

6.1. Changes in Weathering Alkalinity Influx

Over the last 15 million years, Earth's climate has experienced long-term cooling from the mid-Miocene Climatic Optimum to the Pleistocene glaciations of the last 3 Myr. Global ocean temperatures, in both the surface and the deep sea, have dropped by more than 6°C–9°C (Herbert et al., 2016, 2022; Meckler et al., 2022; Super et al., 2020). The causes of this cooling have been contentiously debated (Herbert et al., 2022; Kump & Arthur, 1997; Molnar & Cronin, 2015; Park et al., 2020; Raymo et al., 1988; Rugenstein et al., 2019). Different hypotheses, crucially, predict changes in weathering alkalinity flux in opposite signs.

The often-cited uplift hypothesis suggests that increased chemical weathering in response to active orogeny of the Himalayas drew down atmospheric CO_2 and therefore cooled off the planet (Li et al., 2021; Raymo et al., 1988). This scenario predicts progressive increases in chemical weathering flux over the Neogene and therefore requires increased carbonate burial in the deep sea from the Miocene toward the present.

Alternatively, it has been suggested that the rise of the Himalayas and/or the maritime continent may have increased the weatherability of the Earth (Kump & Arthur, 1997; Molnar & Cronin, 2015; Park et al., 2020; Rugenstein et al., 2019). In this case, global temperature and atmospheric pCO_2 decrease because stronger weathering feedback lowers the steady-state pCO_2 that is needed to maintain the mass balance with CO_2 degassing rates, assuming the source function has been constant.

A deepening of the CCD from the Miocene toward the present indicates that larger seafloor areas became available for carbonate deposition over time. With the (implicit) assumption that carbonate production is constant over time or proportional to the saturation state of the ocean, most previous studies thus conclude that total carbonate burial on the seafloor increased over the last 15 Myr, implying that weathering alkalinity flux has also increased as the global cooling proceeded (Raymo et al., 1988). This interpretation, however, was questioned by Si and Rosenthal (2019), who pointed out that the CCD alone cannot be used as an indicator of past carbonate burial flux because carbonate production at the surface ocean has also changed in inverse correlation to the saturation state of the ocean.

The comparison between 10 Miocene simulations with reconstructed MARc and $CaCO_3$(%) (Figure 2) suggests that scenarios Md (Md+) and Me (Me+) provide a reasonable agreement between the model and data. We thus conclude that from the Middle Miocene to the present, carbonate burial flux at the seafloor and corresponding weathering alkalinity influxes have decreased by ∼30%–45% despite the tendency of the CCD to gently deepen toward the present. This estimate is drastically different from several recent studies, which suggest almost a doubling of pelagic carbonate burial since 15 Ma based on simplified interpretation on the CCD (Dutkiewicz et al., 2019; Müller et al., 2022).

Higher chemical weathering flux in the warm Middle Miocene could come from either higher carbonate weathering or silicate weathering fluxes or both. Based on measurements of dissolved loads from the world's rivers, carbonate weathering likely accounts for ∼50% of modern global chemical weathering fluxes, with the rest mainly from silicate weathering (Gaillardet et al., 1999; Meybeck, 1987). If we assume that the long-term Neogene cooling and pCO_2 decrease result primarily from an increase in the silicate weatherability (Kump & Arthur, 1997; Park et al., 2020; Rugenstein et al., 2019), then CO_2 input from volcanism and corresponding silicate weathering fluxes should all have remained unchanged. Higher weathering alkalinity input (∼30%–45%) in the Miocene will then be attributed to higher carbonate weathering (∼60%–90%) than that of today.

Alternatively, if we assume that the ratio of silicate versus carbonate weathering has remained unchanged over time, our model-data analysis would suggest a 30%–45% decrease in both silicate and carbonate weathering since the Middle Miocene, with the implication of a proportionate decrease in CO_2 degassing. At the first glance, this scenario seems to be inconsistent with the long-held view that seafloor spreading rates have not significantly changed over the course of the Cenozoic. A recent study based on an improved history of seafloor spreading, however, challenges this idea, suggesting that global seafloor spreading rates have decreased by 30%–38% over the last 18 Myr, with a median of 34% (Dalton et al., 2022; Herbert et al., 2022). These new studies thus strongly suggest that long-term diminishments in CO_2 degassing rate have contributed to decreases in chemical weathering fluxes.

In addition to pelagic carbonates, biogenic carbonate production in shelf environments can also affect the global alkalinity budget. One might argue, for instance, that reduced shelf carbonate burial due to lower sea levels since the Miocene can also drive a deepening of the CCD toward the present (illustrated in Figures 1b and 1a). However,

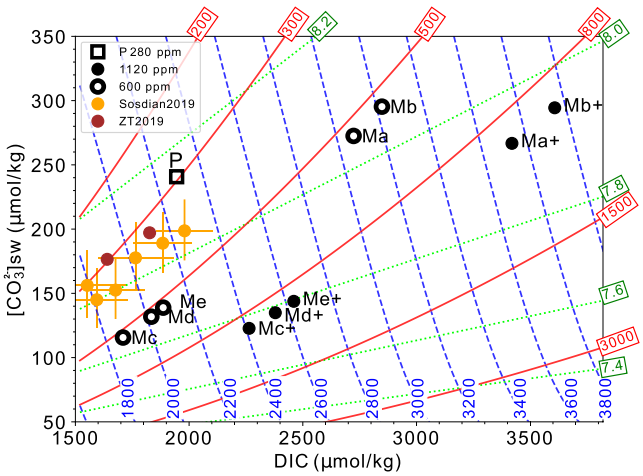

Figure 3. Carbonate chemistry of the Pacific surface ocean (also see Table 2). Blue-dash, green-dot, and red-solid lines indicate total alkalinity (µmol/kg), pH, and pCO_2 (p.p.m.v.), respectively. Dissolved inorganic carbon (*x* axis) and $[CO_3^{2-}]_{sw}$ (*Y* axis) of 10 Miocene scenarios (Ma–Me) and one pre-industry run (P) are averages of the Pacific Ocean in the cGENIE model (65°N–50°S, 125°E–80°W). Orange and brown circles are proxy-based reconstructions from Sosdian, Greenop et al. (2018) and Zeebe and Tyrrell (2019).

it is important to note that this basin-shelf partitioning (Derry, 2022) can only change the CCD, it cannot account for higher Miocene MARc at shallow water depths (above the lysocline) where bottom water has always remained oversaturated. Without changes in carbonate production in the surface ocean, a more corrosive deep ocean would indicate a shallower saturation horizon (Figure 1b) and therefore less carbonate burial at relatively shallow depths. The MARc depth profile, however, indicates the opposite (Figure 2). We thus rule out the basin-shelf hypothesis as first order control of the observed carbonate burial patterns.

Moreover, assuming that carbonate burial on the shelves was higher during the Middle Miocene as a result of higher sea levels, then global decreases in marine carbonate burial rates should be larger than our estimates based on the pelagic records alone, with the further implication that our current estimate of a 30%–45% reduction in global weathering fluxes is conservative.

Another complication to our interpretation involves the cycling of organic materials (C_{org}) in the ocean, which can potentially decouple the CCD from the saturation horizon as well as global marine carbonate burial rates (Greene et al., 2019; Pälike et al., 2012). A recent study using the $\delta^{13}C$ of planktonic foraminifera species suggests that a larger fraction of C_{org} was recycled within the upper ocean during the Miocene relative to today (Boscolo-Galazzo et al., 2021). An increased fraction of labile C_{org} in the Miocene will increase dissolution within the water column and help explain the increased fragmentation of foraminiferal shells in shallow sites (Si & Rosenthal, 2019). It again cannot account for the observation of higher coccolith carbonate burial at shallow depths (Figure 2).

In conclusion, all proxies of chemical weathering have limitations. Carbonate mass accumulation records alone clearly are not sufficient to differentiate carbonate weathering versus silicate weathering and therefore provide no definitive answer to test hypotheses of changes in tectonic degassing versus changes in the weatherability as long-term drivers of atmospheric CO_2 and global climate. Full consideration of the Miocene carbonate cycle might also benefit from simulating the effects of higher shelf carbonate burial or enhanced water column dissolution due to changes in C_{org} cycling. Our analysis, however, does point out the primary role of pelagic carbonate production in driving the vertical distribution of MARc and its importance in understanding and constraining the long-term carbon cycle.

6.2. Relatively Constant Seawater DIC and TA Over the Neogene

Changes in carbonate production not only influence our interpretation of the CCD but also strongly affect seawater carbonate chemistry at steady state, which, as we discuss below, has important implications for long-term changes in DIC, TA, and Ω over the course of the Neogene.

Because atmosphere pCO_2 and the surface ocean are approximately in equilibrium, higher pCO_2 should correspond to elevated DIC and TA, assuming a relatively constant carbonate saturation state (Zeebe & Wolf-Gladrow, 2001). In the Miocene case, this is equivalent to scenario P versus Ma/Ma+. We illustrate this in Figure 3, which averages the carbonate chemistry of the Pacific Ocean in the cGENIE model over the region of 65°N–50°S, 125°E–80°W (Table 2). When the chemical weathering flux remains the same as today (relatively constant saturation), surface ocean DIC (*x*-axis) and TA (blue dash line) must be significantly higher when pCO_2 is also higher. In scenario Ma (600 p.p.m.v.), for instance, DIC and TA are 2,723 and 3,068 µmol/kg, respectively, much higher than modern seawaters. If the Miocene pCO_2 was 1,120 p.p.m.v. (scenario Ma+), DIC and TA would be even higher (Figure 3, Table 2). Furthermore, if we increase weathering alkalinity input by ~30%, the ocean's saturation state, DIC and TA at the steady state will all increase. This is illustrated as the differences between Mb and Ma in Figure 3 (or Mb+ vs. Ma+). Also note that at the steady state, deep sea carbonate burial also increased in case of Mb (Mb+) relative to Ma (Ma+) through a deepening of the CCD (Figure 2).

19449224, 2023, 6, Downloaded from https://agupubs.onlinelibrary.wiley.com/doi/10.1029/2022GB007541, Wiley Online Library on [26/05/2023]. See the Terms and Conditions (https://onlinelibrary.wiley.com/terms-and-conditions) on Wiley Online Library for rules of use; OA articles are governed by the applicable Creative Commons License

19449224, 2023, 6, Downloaded from https://agupubs.onlinelibrary.wiley.com/doi/10.1029/2022GB007541, Wiley Online Library on [26/05/2023]. See the Terms and Conditions (https://onlinelibrary.wiley.com/terms-and-conditions) on Wiley Online Library for rules of use; OA articles are governed by the applicable Creative Commons License

Table 2
Carbonate Chemistry of the Pacific Ocean in the cGENIE Model, Averaged Over the Area Between 65°N–50°S and 125°E–80°W

	P	Ma (Ma+)	Mb (Mb+)	Mc (Mc+)	Md (Md+)	Me (Me+)
$DIC_{\_surface}$	1945	2,723 (3,419)	2,848(3,607)	1709(2,264)	1834 (2,379)	1886 (2,460)
$TA_{\_surface}$	2,289	3,068 (3,728)	3,219 (3,947)	1871(2,408)	2,015(2,538)	2,076 (2,629)
$[CO_3^{2-}]_{surface}$	241	272 (267)	295 (294)	115 (122)	132 (135)	139 (143)
$\Omega_{\_surface}$	5.8	8.5 (8.3)	9.1 (9.1)	3.57 (3.8)	4 (4.1)	4.3 (4.4)
$DIC_{\_deep}$	2,333	3,122 (3,800)	3,249 (3,993)	2,185 (2,707)	2,305 (2,822)	2,356 (2,901)
$TA_{\_deep}$	2,448	3,190 (3,827)	3,324 (4,028)	2,240 (2,721)	2,363 (2,840)	2,415 (2,921)
$[CO_3^{2-}]_{deep}$	87	80.7 (77.8)	87 (85)	55 (50)	59 (54)	60 (56)
$\Omega_{\_deep}$	0.93	1.1 (1.1)	1.2 (1.2)	0.75 (0.76)	0.82 (0.76)	0.83 (0.79)

Note. Unit for DIC, TA, and $[CO_3^{2-}]$ is μmol/kg. Results of the surface ocean are plotted in Figure 3. For the deep Pacific, Ω is calculate at a depth of 4,000 m.

In contrast, reconstructions of DIC and TA using proxy data (Sosdian, Greenop, et al., 2018; Zeebe & Tyrrell, 2019) yield relatively stable or even lower Miocene DIC and TA relative to today (Figure 3, orange and brown circles). What processes have helped maintain relatively invariant DIC and TA pools despite both atmospheric pCO_2 and weathering alkalinity influxes potentially decreasing over the Neogene?

One known process involves secular variations in the calcium concentration of seawater ($[Ca]_{sw}$) (Hain et al., 2015). Over the last 100 Myrs, $[Ca^{2+}]_{sw}$ has dropped from ~50 in the Cretaceous to 10 mmol/kg today (Hardie, 1996; Horita et al., 2002). Assuming chemical weathering fluxes only fluctuated on the order of ±30%, five-fold higher $[Ca^{2+}]_{sw}$ would require proportionately lower $[CO_3^{2-}]_{sw}$ to maintain a relatively stable saturation state of the ocean so that $CaCO_3$ burial can balance the weathering fluxes. Given the steady state pCO_2, a lower $[CO_3^{2-}]_{sw}$ would require lower DIC and TA (Hain et al., 2015). To understand this, one can pick an iso-pCO_2 line in Figure 3, for example, 1,500 p.p.m.v. Sliding along the iso-pCO_2 line toward lower $[CO_3^{2-}]_{sw}$ would require simultaneous decreases in DIC and TA.

Changes in $[Ca^{2+}]_{sw}$ alone, however, cannot account for relatively stable DIC and TA in the Neogene (Figure 3) because a $[Ca^{2+}]_{sw}$ of 12.7 μmol/kg (Zhou et al., 2021) has already been parameterized in our Miocene simulations. Alternatively, we obtain consistent results from scenarios when carbonate production is doubled in the Miocene. Relative to scenario Ma/Ma+, a doubling of carbonate production (Mc/Mc+), all else equal, leads to significantly reduced DIC and TA (Figure 3, Table 2). For our favored scenario Md (Md+) or Me (Me+), increases in weathering alkalinity inputs relative to Mc (Mc+) only add minor changes to TA and DIC. Thus, higher carbonate production appears to be the key factor that maintains relatively constant TA and DIC over time.

How can pelagic carbonate production have such large effects on seawater TA and DIC? The answer lies in the mechanism of carbonate compensation. Increases in carbonate productivities lead to higher carbonate burial at shallow water depths (1,000–3,000 m) (Figure 2). To maintain the alkalinity budget in balance, an equivalent increase in dissolution must occur at depth. This requires a more corrosive deep sea with lower $[CO_3^{2-}]_{sw}$ and Ω. Relative to scenario Mb, doubling carbonate production (scenario Md) results in a decrease in $[CO_3^{2-}]_{sw}$ from ~87 to ~59 μmol/kg and a decrease in Ω from 1.2 to 0.82 (Table 2). Given the steady state pCO_2 of the Middle Miocene (moving alone a red iso-pCO_2 line in Figure 3), a lower mean ocean $[CO_3^{2-}]_{sw}$ (moving down *y* axis) will correspond to lower carbon and alkalinity inventory of the ocean.

Notice that a low $[CO_3^{2-}]_{sw}$ in the deep sea is also associated with low $[CO_3^{2-}]_{sw}$ in the surface ocean (132 μmol/kg in Md), together giving rise to a smaller Miocene vertical $[CO_3^{2-}]_{sw}$ gradient relative to the pre-industrial experiment (Figure S2 in Supporting Information S1). The lower $[CO_3^{2-}]_{sw}$ and thus lower Ω in the surface ocean is interesting (Figure 3, Table 2). It suggests that high $CaCO_3$ production during the Miocene was associated with a less saturated surface ocean, with the implication that biogenic carbonate production (specifically, coccolith production) is highly biologically controlled and not affected simply by the saturation state of the ocean. Instead, Figure 3 and Table 2 point out that Ω (both surface and deep) is a function of biogenic $CaCO_3$ production rates, with higher $CaCO_3$ production driving lower Ω.

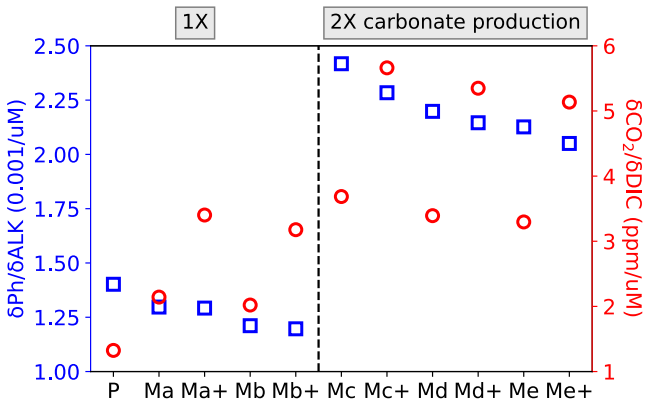

Figure 4. Sensitivity of pH and pCO_2 for per unit change in total alkalinity and dissolved inorganic carbon, respectively. Scenarios to the right have doubled carbonate production. On the *x* axis, different scenarios also correspond to different $[CO_3^{2-}]_{sw}$ and thus different saturation state (Ω) (also see Table 2).

In summary, we conclude that biogenic carbonate production in the surface ocean modulates seawater DIC and TA in a way similar to changes in $[Ca^{2+}]_{sw}$. The relatively constant DIC and TA throughout the Neogene are due to the combined effects of decreases in $[Ca]_{sw}$ and carbonate production as global pCO_2 decreased. Furthermore, significantly increased carbonate production in the pelagic ocean drove lower $[CO_3^{2-}]_{sw}$ in both surface and deep ocean, reducing the whole ocean's carbonate saturation.

6.3. The Choice of Atmospheric pCO_2 Levels

Our modeled DIC and TA (Md and Me, 600 p.p.m.v.) are in close agreement with proxy-based reconstructions for the middle Miocene (Figure 3). However, discrepancies do exist. This primarily reflects the fact that some proxy-based pCO_2 reconstructions suggest mid-Miocene pCO_2 on average ~400 p.p.m.v (Sosdian, Greenop, et al., 2018; Zeebe & Tyrrell, 2019), lower than the 600 and 1,120 p.p.m.v. we used in cGENIE simulation. When the models are forced with higher pCO_2 (Md+ and Me+, 1,120 p.p.m.v.), DIC and TA become higher. Thus, our choice of Miocene pCO_2 does affect the model-data comparison.

Estimating Miocene pCO_2 has been a matter of debate. On one hand, multiple proxies, including Alkenone-SST, TEX86, and clumped isotopes of benthic foraminifera, indicate more than 8°C of warming in the ocean, with the implication of global warming on the magnitude of 12°C (Herbert et al., 2016, 2022; Meckler et al., 2022; Modestou et al., 2020). This requires pCO_2 significantly higher than 400 pmm, given a reasonable guess on Earth System Sensitivity (3°C–6°C warming per doubling of pCO_2) (Knutti et al., 2017; Royer et al., 2007). Reconstructed pCO_2, on the other hand, exhibits large variability ranging from ~200 to above 1,000 p.p.m.v. based on both boron isotope and $\delta^{13}C$ of alkenone biomarkers (Rae et al., 2021; Sosdian, Greenop, et al., 2018; Stoll et al., 2019; Super et al., 2018; Tanner et al., 2020).

One possible argument is that the ice albedo that comes into play in the last 3 Myr tends to enhance effective climate sensitivity at low pCO_2. As a result, a small increase in pCO_2 from 280 p.p.m.v might have a large effect on equilibrium climate if the Earth becomes ice-free (Ring et al., 2022). However, available Miocene simulations with less than 600 p.p.m.v cannot produce the magnitude of mid-Miocene warming (Burls et al., 2021). We thus consider that 400 p.p.m.v. pCO_2 is unlikely and choose 600 p.p.m.v. as the low end of our simulations, which is also more consistent with recently updated pCO_2 estimates (Rae et al., 2021; Stoll et al., 2019; Tanner et al., 2020). On the other hand, Crichton et al. (2021) suggested that a pCO_2 value of 1,120 p.p.m.v. is necessary to simulate the observed Miocene warming in cGENIE. A recent revision on the alkenone-based pCO_2 calibration also suggests that Miocene pCO_2 of >1,000 p.p.m.v. is within the uncertainty of the proxy calibration (Tanner et al., 2020). If this is true, we may have underestimated Miocene carbonate production in cGENIE simulations by omitting potential changes in shelf carbonate deposits (see discussion in Section 6.1). Also note that higher neritic carbonate production and burial during the Miocene highstand would require lower DIC and TA than inferred in Figure 3.

6.4. Reduced Buffering Capacity of the Ocean

Another consequence of enhanced carbonate production is a large decrease in the ocean's buffering capacity. Seawater is a relatively well-buffered solution that is capable of resisting changes in acidity. Several indices have been used to quantify seawater buffering capacity (Middelburg et al., 2020). Here we compare the sensitivity of pH to per unit change in TA (dpH/dTA) and the sensitivity of pCO_2 to per unit change in DIC (dCO_2/dDIC) (also known as inverse buffer factor, Figure 4).

For simulations with the same weathering flux and carbonate production but different pCO_2 values, pCO_2 is more sensitive to change in DIC when background pCO_2 is higher (e.g., Ma vs. Ma+). On the other hand, increases in chemical weathering flux show minor effects on either dpH/dTA or dCO_2/dDIC (Ma vs. Mb). Large decreases in the buffering capacity, however, are observed in simulations with doubled (2X) carbonate production.

19449224, 2023, 6, Downloaded from https://agupubs.onlinelibrary.wiley.com/doi/10.1029/2022GB007541, Wiley Online Library on [26/05/2023]. See the Terms and Conditions (https://onlinelibrary.wiley.com/terms-and-conditions) on Wiley Online Library for rules of use; OA articles are governed by the applicable Creative Commons License

19449224, 2023, 6, Downloaded from https://agupubs.onlinelibrary.wiley.com/doi/10.1029/2022GB007541, Wiley Online Library on [26/05/2023]. See the Terms and Conditions (https://onlinelibrary.wiley.com/terms-and-conditions) on Wiley Online Library for rules of use; OA articles are governed by the applicable Creative Commons License

As discussed above, enhanced carbonate production requires lower $[CO_3^{2-}]_{sw}$ in order to maintain the alkalinity budget in balance, namely, weathering alkalinity input being equal to carbonate burial flux. Comparing scenarios Ma versus Mc, modeled deep Pacific $[CO_3^{2-}]_{sw}$ is ~81 and 55 μmol/kg, respectively (Table 2, Figure S2 in Supporting Information S1). At steady state, this implies smaller DIC (3,122 vs. 2,185 μmol/kg) and TA (3,190 vs. 2,240 μmol/kg) of the ocean (Table 2). Qualitatively, the buffering capacity of seawater in relation to the reservoir size can be illustrated in Figure 3. On the right-hand side of the figure, iso-pCO_2 lines pCO_2 = 800 and pCO_2 = 1,500 are widely separated, while they are more closely spaced on the left-hand side of the figure. As a result, given a perturbation in the DIC, pCO_2 will change more when the DIC is relatively small. A similar argument can be applied to dpH/dTA (green dotted line and blue dash line). The implication would be that for timescales <1 Myr, a reduced buffering capacity would allow for more short-term changes in pCO_2 forced by a variety of processes.

6.5. A Possible Cause of the Neogene Decrease in Carbonate Production

The higher carbonate production during the mid-Miocene is entirely driven by coccolithophorid paleoecology (Si & Rosenthal, 2019; Suchéras-Marx & Henderiks, 2014). Unlike foraminifera, coccolithophores calcify inside the cell (Bolton & Stoll, 2013 and references therein). Similar to other marine phytoplankton (Hopkinson et al., 2011; Reinfelder, 2011), recent studies suggest that due to the strong demand for carbon for photosynthesis, dissolved carbon supplies from extracellular seawater to intracellular loci of photosynthesis are likely limited by the concentration of dissolved $[CO_2]_{aq}$ in the seawater (Bolton & Stoll, 2013; Hermoso et al., 2015; McClelland et al., 2016). When pCO_2 is low, dissolved $[CO_2]_{aq}$ in seawater may have become a limiting nutrient for the growth of coccolithophores rather than simply a stressor. These inferences are partially supported by the study of Bolton et al. (2016), who suggested reduced calcification in the last 15 Myr as pCO_2 decreased.

On the other hand, measurements of the degree of calcification cannot directly be translated to global pelagic carbonate productivity. In the modern ocean, smaller coccolithophores tend to be more numerically abundant, contributing more to carbonate fluxes than their larger counterparts (e.g., Iglesias-Rodriguez et al., 2008). Bigger coccolithophore cells with higher PIC/POC ratios (Bolton et al., 2016) thus do not necessarily indicate higher MARc. Other factors such as the evolutionary adaptions of coccolithophorid species in the last few million years (Aubry, 2007) as well as long-term changes in nutrient recycling of the ocean (Boscolo-Galazzo et al., 2021) may have all played a role in driving global coccolith productivity.

Although our studies on deep-time records reveal a calcification pattern that is apparently contradictory to many laboratory-based studies, there actually exist hints in the literature that reported increased calcification under elevated pCO_2 (and lower Ω) in modern species (Benner et al., 2013; Iglesias-Rodriguez et al., 2008; Krumhardt et al., 2016; McClelland et al., 2016; Rivero-Calle et al., 2015; Smith et al., 2012). By exposing *Emiliania huxleyi* under prolonged pCO_2 forcing, for instance, Lohbeck et al. found that relative to those kept at ambient conditions, adapted strains after 500 asexual generations exhibited higher growth rates when tested under ocean acidification conditions (Lohbeck et al., 2012). The short generation time and diverse phenotypes ranging from completely non-calcifying to heavily calcified strains in some coccolithophorid species may allow for their rapid adaption to environmental changes.

Studies based on paleo-records and culturing experiments both have their own limitations. The goal of this discussion is not to rule out one hypothesis or another but instead to emphasize the complex relationship of coccolithophorid calcification to climate changes. Beyond the Middle Miocene examined here, geological records also provide other instances of coccolithophorid responses to elevated pCO_2 and extreme greenhouse climate, including robustly calcified coccoliths during the Eocene (Claxton et al., 2022) and the massive pelagic chalk deposits during the Cretaceous (*creta* = chalk). Future studies on these paleo-archives may provide further insights into the evolutionary adaptions of coccolithophores to past extreme warm climate.

7. Conclusion

In this study, we present a model-data comparison to demonstrate that global pelagic carbonate production was approximately doubled in the Middle Miocene when pCO_2 and temperature were both higher. Given the constraints of the CCD and MARc, we infer that global pelagic carbonate burial and chemical weathering flux were ~30%–45% higher than pre-industrial levels. We also show that the relatively constant or lower

19449224, 2023, 6, Downloaded from https://agupubs.onlinelibrary.wiley.com/doi/10.1029/2022GB007541, Wiley Online Library on [26/05/2023]. See the Terms and Conditions (https://onlinelibrary.wiley.com/terms-and-conditions) on Wiley Online Library for rules of use; OA articles are governed by the applicable Creative Commons License

than pre-industrial carbon (DIC) and alkalinity (TA) inventory of the ocean in the Miocene, as demonstrated in $\delta^{11}B$-based reconstructions, are likely the results of both higher seawater $[Ca^{2+}]_{sw}$ and higher calcium carbonate production which result in lower $[CO_3^{2-}]_{sw}$ and counteract the increase due to higher alkalinity weathering flux and elevated atmospheric pCO_2. In contrast to previous studies, which suggest a relatively constant saturation state of the ocean over geological time, higher carbonate production in the Miocene reduced Ω in both the surface and the deep ocean. Higher carbonate production also significantly reduced the buffering capacity of the Miocene Ocean (sensitivity of pH, pCO_2 to perturbation in TA, DIC). This positive correlation between the biologically driven calcification in the ocean and pCO_2 on long timescale may have acted as positive feedback to augment the decrease in atmospheric pCO_2 in increasing ocean's buffering capacity from the Miocene to the present.

Data Availability Statement

cGENIE used for this study has open access at https://doi.org/10.5281/zenodo.4615662 (Ridgwell et al., 2021). Base configuration of our Miocene simulation is available in the supporting materials of Crichton et al. (2021). Modified configuration files used for this study are available as online supplementary materials. Mass Accumulation Rates of Carbonate in Figure 2 are from Si and Rosenthal (2019) and can be found in the NOAA data repository https://www.ncei.noaa.gov/pub/data/paleo/ or by contacting the authors.

Acknowledgments
This work is partially supported by NSF 1635127 to T. Herbert, NSF-OCE 2202760 to W. Si and T. Herbert, and OCE-BSF-1634573 to Y. Rosenthal. We also thank the Center for Computation and Visualization, Brown University, for providing computing resources, and A. Ridgwell for training W. Si to use cGENIE under the support of the NSF-funded Research Coordination Network (RCN) for "Improving Reconstructions of Cenozoic pCO_2 Change." We also thank two reviewers for their constructive comments, which significantly improved the manuscript.

References

Albright, R., Takeshita, Y., Koweek, D. A., Ninokawa, A., Wolfe, K., Rivlin, T., et al. (2018). Carbon dioxide addition to coral reef waters suppresses net community calcification. *Nature*, *555*(7697), 516–519. https://doi.org/10.1038/nature25968

Aubry, M. P. (2007). A major Pliocene coccolithophore turnover: Change in morphological strategy in the photic zone. *Large Ecosystem Perturbations: Causes and Consequences*, *424*, 25–51. https://doi.org/10.1130/2007.2424(02

Bach, L. T., Bauke, C., Meier, K., Riebesell, U., & Schulz, K. G. (2012). Influence of changing carbonate chemistry on morphology and weight of coccoliths formed by *Emiliania huxleyi*. *Biogeosciences*, *9*(8), 3449–3463. https://doi.org/10.5194/bg-9-3449-2012

Benner, I., Diner, R. E., Lefebvre, S. C., Li, D., Komada, T., Carpenter, E. J., & Stillman, J. H. (2013). *Emiliania huxleyi* increases calcification but not expression of calcification-related genes in long-term exposure to elevated temperature and pCO_2. *Philosophical Transactions of the Royal Society B: Biological Sciences*, *368*(1627), 20130049. https://doi.org/10.1098/rstb.2013.0049

Berelson, W. M., Balch, W. M., Najjar, R., Feely, R. A., Sabine, C., & Lee, K. (2007). Relating estimates of $CaCO_3$ production, export, and dissolution in the water column to measurements of $CaCO_3$ rain into sediment traps and dissolution on the sea floor: A revised global carbonate budget. *Global Biogeochemical Cycles*, *21*(1), GB1024. https://doi.org/10.1029/2006gb002803

Berner, R. A., & Caldeira, K. (1997). The need for mass balance and feedback in the geochemical carbon cycle. *Geology*, *25*(10), 955–956. https://doi.org/10.1130/0091-7613(1997)025<0955:Tnfmba>2.3.Co;2

Berner, R. A., & Kothavala, Z. (2001). GEOCARB III: A revised model of atmospheric CO_2 over phanerozoic time. *American Journal of Science*, *301*(2), 182–204. https://doi.org/10.2475/ajs.301.2.182

Berner, R. A., Lasaga, A. C., & Garrels, R. M. (1983). The carbonate-silicate geochemical cycle and its effect on atmospheric carbon dioxide over the past 100 million years. *American Journal of Science*, *283*(7), 641–683. https://doi.org/10.2475/ajs.283.7.641

Bijma, J., Faber, W. W., & Hemleben, C. (1990). Temperature and salinity limits for growth and survival of some planktonic foraminifers in laboratory cultures. *Journal of Foraminiferal Research*, *20*(2), 95–116. https://doi.org/10.2113/gsjfr.20.2.95

Bolton, C. T., Hernández-Sánchez, M. T., Fuertes, M.-A., González-Lemos, S., Abrevaya, L., Mendez-Vicente, A., et al. (2016). Decrease in coccolithophore calcification and CO_2 since the middle Miocene. *Nature Communications*, *7*(1), 10284. https://doi.org/10.1038/ncomms10284

Bolton, C. T., & Stoll, H. M. (2013). Late Miocene threshold response of marine algae to carbon dioxide limitation. *Nature*, *500*(7464), 558–62. https://doi.org/10.1038/nature12448

Boscolo-Galazzo, F., Crichton, K. A., Ridgwell, A., Mawbey, E. M., Wade, B. S., & Pearson, P. N. (2021). Temperature controls carbon cycling and biological evolution in the ocean twilight zone. *Science*, *371*(6534), 1148–1152. https://doi.org/10.1126/science.abb6643

Boudreau, B. P., Middelburg, J. J., Sluijs, A., & van der Ploeg, R. (2019). Secular variations in the carbonate chemistry of the oceans over the Cenozoic. *Earth and Planetary Science Letters*, *512*, 194–206. https://doi.org/10.1016/j.epsl.2019.02.004

Broecker, W. S. (1971). A kinetic model for the chemical composition of sea water. *Quaternary Research*, *1*(2), 188–207. https://doi.org/10.1016/0033-5894(71)90041-x

Broecker, W. S. (2003). The oceanic $CaCO_3$ cycle. *Treatise on Geochemistry*, *6*, 625.

Broecker, W. S., & Sanyal, A. (1998). Does atmospheric CO_2 police the rate of chemical weathering? *Global Biogeochemical Cycles*, *12*(3), 403–408. https://doi.org/10.1029/98gb01927

Burls, N. J., Bradshaw, C., De Boer, A. M., Herold, N., Huber, M., Pound, M., et al. (2021). Simulating Miocene warmth: Insights from an opportunistic multi-model ensemble (MioMIP1). *Paleoceanography and Paleoclimatology*, *36*(5), e2020PA004054. https://doi.org/10.1029/2020PA004054

Cai, W., Guo, X., Chen, C., Dai, M., Zhang, L., Zhai, W., et al. (2008). A comparative overview of weathering intensity and HCO_3− flux in the world's major rivers with emphasis on the Changjiang, Huanghe, Zhujiang (Pearl) and Mississippi Rivers. *Continental Shelf Research*, *28*(12), 1538–1549. https://doi.org/10.1016/j.csr.2007.10.014

Campbell, S. M., Moucha, R., Derry, L. A., & Raymo, M. E. (2018). Effects of dynamic topography on the Cenozoic carbonate compensation depth. *Geochemistry, Geophysics, Geosystems*, *19*(4), 1025–1034. https://doi.org/10.1002/2017gc007386

Claxton, L., McClelland, H., Hermoso, M., & Rickaby, R. (2022). Eocene emergence of highly calcifying coccolithophores despite declining atmospheric CO_2. *Nature Geoscience*, *15*(10), 826–831. https://doi.org/10.1038/s41561-022-01006-0

Crichton, K. A., Ridgwell, A., Lunt, D. J., Farnsworth, A., & Pearson, P. N. (2021). Data-constrained assessment of ocean circulation changes since the middle Miocene in an Earth system model. *Climate of the Past Discussions*, *2021*, 1–36. https://doi.org/10.5194/cp-2019-151

Dalton, C. A., Wilson, D. S., & Herbert, T. D. (2022). Evidence for a global slowdown in seafloor spreading since 15 Ma. *Geophysical Research Letters*, *49*(6), e2022GL097937. https://doi.org/10.1029/2022gl097937

de Nooijer, L. J., Toyofuku, T., & Kitazato, H. (2009). Foraminifera promote calcification by elevating their intracellular pH. *Proceedings of the National Academy of Sciences of the United States of America*, *106*(36), 15374–15378. https://doi.org/10.1073/pnas.0904306106
Derry, L. A. (2022). Carbonate weathering, CO_2 redistribution, and Neogene CCD and pCO_2 evolution. *Earth and Planetary Science Letters*, *597*, 117801. https://doi.org/10.1016/j.epsl.2022.117801
Dutkiewicz, A., & Müller, R. D. (2021). The carbonate compensation depth in the South Atlantic Ocean since the late Cretaceous. *Geology*, *49*(7), 873–878. https://doi.org/10.1130/g48404.1
Dutkiewicz, A., Müller, R. D., Cannon, J., Vaughan, S., & Zahirovic, S. (2019). Sequestration and subduction of deep-sea carbonate in the global ocean since the Early Cretaceous. *Geology*, *47*(1), 91–94. https://doi.org/10.1130/g45424.1
Fabry, V. J., Seibel, B. A., Feely, R. A., & Orr, J. C. (2008). Impacts of ocean acidification on marine fauna and ecosystem processes. *ICES Journal of Marine Science*, *65*(3), 414–432. https://doi.org/10.1093/icesjms/fsn048
Farrell, J. W., & Prell, W. L. (1991). Pacific $CaCO_3$ preservation and $\delta^{18}O$ since 4 Ma: Paleoceanic and paleoclimatic implications. *Paleoceanography*, *6*(4), 485–498. https://doi.org/10.1029/91pa00877
Feely, R. A., Sabine, C. L., Lee, K., Berelson, W., Kleypas, J., Fabry, V. J., & Millero, F. J. (2004). Impact of anthropogenic CO_2 on the $CaCO_3$ system in the oceans. *Science*, *305*(5682), 362–366. https://doi.org/10.1126/science.1097329
Gaillardet, J., Dupré, B., Louvat, P., & Allègre, C. J. (1999). Global silicate weathering and CO_2 consumption rates deduced from the chemistry of large rivers. *Chemical Geology*, *159*(1–4), 3–30. https://doi.org/10.1016/s0009-2541(99)00031-5
Greene, S., Ridgwell, A., Kirtland Turner, S., Schmidt, D. N., Pälike, H., Thomas, E., et al. (2019). Early Cenozoic decoupling of climate and carbonate compensation depth trends. *Paleoceanography and Paleoclimatology*, *34*(6), 930–945. https://doi.org/10.1029/2019pa003601
Hain, M. P., Sigman, D. M., Higgins, J. A., & Haug, G. H. (2015). The effects of secular calcium and magnesium concentration changes on the thermodynamics of seawater acid/base chemistry: Implications for Eocene and Cretaceous ocean carbon chemistry and buffering. *Global Biogeochemical Cycles*, *29*(5), 517–533. https://doi.org/10.1002/2014gb004986
Hardie, L. A. (1996). Secular variation in seawater chemistry: An explanation for the coupled secular variation in the mineralogies of marine limestones and potash evaporites over the past 600 my. *Geology*, *24*(3), 279–283. https://doi.org/10.1130/0091-7613(1996)024<0279:svisca>2.3.co;2
Herbert, T. D., Dalton, C. A., Liu, Z., Salazar, A., Si, W., & Wilson, D. S. (2022). Tectonic degassing drove global temperature trends since 20 Ma. *Science*, *377*(6601), 116–119. https://doi.org/10.1126/science.abl4353
Herbert, T. D., Lawrence, K. T., Tzanova, A., Peterson, L. C., Caballero-Gill, R., & Kelly, C. S. (2016). Late Miocene global cooling and the rise of modern ecosystems. *Nature Geoscience*, *9*(11), 843–847. https://doi.org/10.1038/ngeo2813
Hermoso, M., Chan, I., McClelland, H., Heureux, A., & Rickaby, R. (2015). Vanishing coccolith vital effects with alleviated CO_2 limitation. *Biogeosciences Discussions*, *12*(18), 15835–15866. https://doi.org/10.5194/bgd-12-15835-2015
Hoegh-Guldberg, O., Mumby, P. J., Hooten, A. J., Steneck, R. S., Greenfield, P., Gomez, E., et al. (2007). Coral reefs under rapid climate change and ocean acidification. *Science*, *318*(5857), 1737–1742. https://doi.org/10.1126/science.1152509
Hönisch, B., Ridgwell, A., Schmidt, D. N., Thomas, E., Gibbs, S. J., Sluijs, A., et al. (2012). The geological record of ocean acidification. *Science*, *335*(6072), 1058–1063. https://doi.org/10.1126/science.1208277
Hopkinson, B. M., Dupont, C. L., Allen, A. E., & Morel, F. M. (2011). Efficiency of the CO_2-concentrating mechanism of diatoms. *Proceedings of the National Academy of Sciences of the United States of America*, *108*(10), 3830–3837. https://doi.org/10.1073/pnas.1018062108
Horita, J., Zimmermann, H., & Holland, H. D. (2002). Chemical evolution of seawater during the Phanerozoic: Implications from the record of marine evaporites. *Geochimica et Cosmochimica Acta*, *66*(21), 3733–3756. https://doi.org/10.1016/s0016-7037(01)00884-5
Iglesias-Rodriguez, M. D., Halloran, P. R., Rickaby, R. E., Hall, I. R., Colmenero-Hidalgo, E., Gittins, J. R., et al. (2008). Phytoplankton calcification in a high-CO_2 world. *Science*, *320*(5874), 336–340. https://doi.org/10.1126/science.1154122
Jin, X., Gruber, N., Dunne, J. P., Sarmiento, J. L., & Armstrong, R. A. (2006). Diagnosing the contribution of phytoplankton functional groups to the production and export of particulate organic carbon, $CaCO_3$, and opal from global nutrient and alkalinity distributions. *Global Biogeochemical Cycles*, *20*(2), GB2015. https://doi.org/10.1029/2005gb002532
Jokiel, P., Rodgers, K., Kuffner, I., Andersson, A., Cox, E., & Mackenzie, F. (2008). Ocean acidification and calcifying reef organisms: A mesocosm investigation. *Coral Reefs*, *27*(3), 473–483. https://doi.org/10.1007/s00338-008-0380-9
Kleypas, J. A., Feely, R. A., Fabry, V. J., Langdon, C., Sabine, C. L., & Robbins, L. L. (2005). *Impacts of ocean acidification on coral reefs and other marine calcifiers: A guide for future research* (Vol. 18, p. 20). Citeseer.
Knutti, R., Rugenstein, M. A., & Hegerl, G. C. (2017). Beyond equilibrium climate sensitivity. *Nature Geoscience*, *10*(10), 727–736. https://doi.org/10.1038/ngeo3017
Krissansen-Totton, J., & Catling, D. C. (2017). Constraining climate sensitivity and continental versus seafloor weathering using an inverse geological carbon cycle model. *Nature Communications*, *8*(1), 15423. https://doi.org/10.1038/ncomms15423
Krumhardt, K. M., Lovenduski, N. S., Freeman, N. M., & Bates, N. R. (2016). Apparent increase in coccolithophore abundance in the subtropical North Atlantic from 1990 to 2014. *Biogeosciences*, *13*(4), 1163–1177. https://doi.org/10.5194/bg-13-1163-2016
Kump, L. R., & Arthur, M. A. (1997). Global chemical erosion during the Cenozoic: Weatherability balances the budgets. In *Tectonic uplift and climate change* (pp. 399–426). Springer.
Lauvset, S. K., Lange, N., Tanhua, T., Bittig, H. C., Olsen, A., Kozyr, A., et al. (2021). An updated version of the global interior ocean biogeochemical data product, GLODAPv2. 2021. *Earth System Science Data*, *13*(12), 5565–5589. https://doi.org/10.5194/essd-13-5565-2021
Lee, K. (2001). Global net community production estimated from the annual cycle of surface water total dissolved inorganic carbon. *Limnology and Oceanography*, *46*(6), 1287–1297. https://doi.org/10.4319/lo.2001.46.6.1287
Li, S., Goldstein, S., & Raymo, M. (2021). Neogene continental denudation and the beryllium conundrum. *Proceedings of the National Academy of Sciences of the United States of America*, *118*(42), e2026456118. https://doi.org/10.1073/pnas.2026456118
Lohbeck, K. T., Riebesell, U., & Reusch, T. B. (2012). Adaptive evolution of a key phytoplankton species to ocean acidification. *Nature Geoscience*, *5*(5), 346–351. https://doi.org/10.1038/ngeo1441
Lombard, F., da Rocha, R. E., Bijma, J., & Gattuso, J.-P. (2010). Effect of carbonate ion concentration and irradiance on calcification in planktonic foraminifera. *Biogeosciences*, *7*(1), 247–255. https://doi.org/10.5194/bg-7-247-2010
Lyle, M. (2003). Neogene carbonate burial in the Pacific Ocean. *Paleoceanography*, *18*(3), 1059. https://doi.org/10.1029/2002pa000777
McClelland, H., Barbarin, N., Beaufort, L., Hermoso, M., Ferretti, P., Greaves, M., & Rickaby, R. (2016). Calcification response of a key phytoplankton family to millennial-scale environmental change. *Scientific Reports*, *6*(1), 1–11. https://doi.org/10.1038/srep34263
Meckler, A. N., Sexton, P., Piasecki, A., Leutert, T., Marquardt, J., Ziegler, M., et al. (2022). Cenozoic evolution of deep ocean temperature from clumped isotope thermometry. *Science*, *377*(6601), 86–90. https://doi.org/10.1126/science.abk0604
Meybeck, M. (1987). Global chemical weathering of surficial rocks estimated from river dissolved loads. *American Journal of Science*, *287*(5), 401–428. https://doi.org/10.2475/ajs.287.5.401

19449224, 2023, 6, Downloaded from https://agupubs.onlinelibrary.wiley.com/doi/10.1029/2022GB007541, Wiley Online Library on [26/05/2023]. See the Terms and Conditions (https://onlinelibrary.wiley.com/terms-and-conditions) on Wiley Online Library for rules of use; OA articles are governed by the applicable Creative Commons License

Meyer, J., & Riebesell, U. (2015). Reviews and syntheses: Responses of coccolithophores to ocean acidification: A meta-analysis. *Biogeosciences*, *12*(6), 1671–1682. https://doi.org/10.5194/bg-12-1671-2015

Middelburg, J. J., Soetaert, K., & Hagens, M. (2020). Ocean alkalinity, buffering and biogeochemical processes. *Reviews of Geophysics*, *58*(3), e2019RG000681. https://doi.org/10.1029/2019rg000681

Milliman, J. D. (1993). Production and accumulation of calcium-carbonate in the ocean - Budget of a nonsteady state. *Global Biogeochemical Cycles*, *7*(4), 927–957. https://doi.org/10.1029/93gb02524

Modestou, S. E., Leutert, T. J., Fernandez, A., Lear, C. H., & Meckler, A. N. (2020). Warm middle Miocene Indian Ocean bottom water temperatures: Comparison of clumped isotope and Mg/Ca-based estimates. *Paleoceanography and Paleoclimatology*, *35*(11), e2020PA003927. https://doi.org/10.1029/2020pa003927

Molnar, P., & Cronin, T. W. (2015). Growth of the maritime continent and its possible contribution to recurring ice ages. *Paleoceanography*, *30*(3), 196–225. https://doi.org/10.1002/2014pa002752

Müller, R. D., Mather, B., Dutkiewicz, A., Keller, T., Merdith, A., Gonzalez, C. M., et al. (2022). Evolution of Earth's tectonic carbon conveyor belt. *Nature*, *605*(7911), 629–639. https://doi.org/10.1038/s41586-022-04420-x

Orr, J. C., Fabry, V. J., Aumont, O., Bopp, L., Doney, S. C., Feely, R. A., et al. (2005). Anthropogenic ocean acidification over the twenty-first century and its impact on calcifying organisms. *Nature*, *437*(7059), 681–686. https://doi.org/10.1038/nature04095

Pälike, H., Lyle, M., Nishi, H., Raffi, I., Ridgwell, A., Gamage, K., et al. (2012). A Cenozoic record of the equatorial Pacific carbonate compensation depth. *Nature*, *488*(7413), 609–14. https://doi.org/10.1038/nature11360

Park, Y., Maffre, P., Goddéris, Y., Macdonald, F. A., Anttila, E. S., & Swanson-Hysell, N. L. (2020). Emergence of the Southeast Asian islands as a driver for Neogene cooling. *Proceedings of the National Academy of Sciences of the United States of America*, *117*(41), 25319–25326. https://doi.org/10.1073/pnas.2011033117

Rae, J. W., Zhang, Y. G., Liu, X., Foster, G. L., Stoll, H. M., & Whiteford, R. D. (2021). Atmospheric CO_2 over the past 66 million years from marine archives. *Annual Review of Earth and Planetary Sciences*, *49*(1), 609–641. https://doi.org/10.1146/annurev-earth-082420-063026

Raven, J., Caldeira, K., Elderfield, H., Hoegh-Guldberg, O., Liss, P., Riebesell, U., et al. (2005). *Ocean acidification due to increasing atmospheric carbon dioxide*. The Royal Society.

Raymo, M. E., Ruddiman, W. F., & Froelich, P. N. (1988). Influence of late Cenozoic mountain building on ocean geochemical cycles. *Geology*, *16*(7), 649–653. https://doi.org/10.1130/0091-7613(1988)016<0649:Iolcmb>2.3.Co;2

Reinfelder, J. R. (2011). Carbon concentrating mechanisms in eukaryotic marine phytoplankton. *Annual Review of Marine Science*, *3*(1), 291–315. https://doi.org/10.1146/annurev-marine-120709-142720

Reynaud, S., Leclercq, N., Romaine-Lioud, S., Ferrier-Pagés, C., Jaubert, J., & Gattuso, J. (2003). Interacting effects of CO_2 partial pressure and temperature on photosynthesis and calcification in a scleractinian coral. *Global Change Biology*, *9*(11), 1660–1668. https://doi.org/10.1046/j.1365-2486.2003.00678.x

Ridgwell, A., DomHu, Peterson, C., Ward, B., Evansmn, S., & Jones, R. (2021). derpycode/muffindoc: (v0.9.20). https://doi.org/10.5281/zenodo.4615662

Ridgwell, A., & Hargreaves, J. (2007). Regulation of atmospheric CO_2 by deep-sea sediments in an Earth system model. *Global Biogeochemical Cycles*, *21*(2), GB2008. https://doi.org/10.1029/2006gb002764

Ridgwell, A., & Zeebe, R. E. (2005). The role of the global carbonate cycle in the regulation and evolution of the Earth system. *Earth and Planetary Science Letters*, *234*(3–4), 299–315. https://doi.org/10.1016/j.epsl.2005.03.006

Riebesell, U., Zondervan, I., Rost, B., Tortell, P. D., Zeebe, R. E., & Morel, F. M. (2000). Reduced calcification of marine plankton in response to increased atmospheric CO_2. *Nature*, *407*(6802), 364–367. https://doi.org/10.1038/35030078

Ring, S. J., Mutz, S. G., & Ehlers, T. A. (2022). Cenozoic proxy constraints on Earth system sensitivity to greenhouse gases. *Paleoceanography and Paleoclimatology*, *37*(12), e2021PA004364. https://doi.org/10.1029/2021pa004364

Rivero-Calle, S., Gnanadesikan, A., Del Castillo, C. E., Balch, W. M., & Guikema, S. D. (2015). Multidecadal increase in North Atlantic coccolithophores and the potential role of rising CO_2. *Science*, *350*(6267), 1533–7. https://doi.org/10.1126/science.aaa8026

Royer, D. L., Berner, R. A., & Park, J. (2007). Climate sensitivity constrained by CO_2 concentrations over the past 420 million years. *Nature*, *446*(7135), 530–532. https://doi.org/10.1038/nature05699

Rugenstein, J. K. C., Ibarra, D. E., & von Blanckenburg, F. (2019). Neogene cooling driven by land surface reactivity rather than increased weathering fluxes. *Nature*, *571*(7763), 99–102. https://doi.org/10.1038/s41586-019-1332-y

Si, W., & Rosenthal, Y. (2019). Reduced continental weathering and marine calcification linked to late Neogene decline in atmospheric CO_2. *Nature Geoscience*, *12*(10), 833–838. https://doi.org/10.1038/s41561-019-0450-3

Slater, S. M., Bown, P., Twitchett, R. J., Danise, S., & Vajda, V. (2022). Global record of "ghost" nannofossils reveals plankton resilience to high CO_2 and warming. *Science*, *376*(6595), 853–856. https://doi.org/10.1126/science.abm7330

Smith, H. E., Tyrrell, T., Charalampopoulou, A., Dumousseaud, C., Legge, O. J., Birchenough, S., et al. (2012). Predominance of heavily calcified coccolithophores at low $CaCO_3$ saturation during winter in the Bay of Biscay. *Proceedings of the National Academy of Sciences of the United States of America*, *109*(23), 8845–8849. https://doi.org/10.1073/pnas.1117508109

Sosdian, S. M., Greenop, R., Hain, M., Foster, G. L., Pearson, P. N., & Lear, C. H. (2018). Constraining the evolution of Neogene ocean carbonate chemistry using the boron isotope pH proxy. *Earth and Planetary Science Letters*, *498*, 362–376. https://doi.org/10.1016/j.epsl.2018.06.017

Sosdian, S. M., Rosenthal, Y., & Toggweiler, J. (2018). Deep Atlantic carbonate ion and $CaCO_3$ compensation during the ice ages. *Paleoceanography and Paleoclimatology*, *33*(6), 546–562. https://doi.org/10.1029/2017pa003312

Stoll, H. M., Guitian, J., Hernandez-Almeida, I., Mejia, L. M., Phelps, S., Polissar, P., et al. (2019). Upregulation of phytoplankton carbon concentrating mechanisms during low CO_2 glacial periods and implications for the phytoplankton pCO_2 proxy. *Quaternary Science Reviews*, *208*, 1–20. https://doi.org/10.1016/j.quascirev.2019.01.012

Suchéras-Marx, B., & Henderiks, J. (2014). Downsizing the pelagic carbonate factory: Impacts of calcareous nannoplankton evolution on carbonate burial over the past 17 million years. *Global and Planetary Change*, *123*, 97–109. https://doi.org/10.1016/j.gloplacha.2014.10.015

Sulpis, O., Boudreau, B. P., Mucci, A., Jenkins, C., Trossman, D. S., Arbic, B. K., & Key, R. M. (2018). Current $CaCO_3$ dissolution at the seafloor caused by anthropogenic CO_2. *Proceedings of the National Academy of Sciences of the United States of America*, *115*(46), 11700–11705. https://doi.org/10.1073/pnas.1804250115

Super, J. R., Thomas, E., Pagani, M., Huber, M., O'Brien, C., & Hull, P. M. (2018). North Atlantic temperature and pCO_2 coupling in the early-middle Miocene. *Geology*, *46*(6), 519–522. https://doi.org/10.1130/g40228.1

Super, J. R., Thomas, E., Pagani, M., Huber, M., O'Brien, C. L., & Hull, P. M. (2020). Miocene evolution of North Atlantic sea surface temperature. *Paleoceanography and Paleoclimatology*, *35*(5), e2019PA003748. https://doi.org/10.1029/2019pa003748

Tanner, T., Hernández-Almeida, I., Drury, A. J., Guitián, J., & Stoll, H. (2020). Decreasing atmospheric CO_2 during the late miocene cooling. *Paleoceanography and Paleoclimatology*, *35*(12), e2020PA003925. https://doi.org/10.1029/2020pa003925

19449224, 2023, 6, Downloaded from https://agupubs.onlinelibrary.wiley.com/doi/10.1029/2022GB007541, Wiley Online Library on [26/05/2023]. See the Terms and Conditions (https://onlinelibrary.wiley.com/terms-and-conditions) on Wiley Online Library for rules of use; OA articles are governed by the applicable Creative Commons License

Toggweiler, J., & Sarmiento, J. (1985). Glacial to interglacial changes in atmospheric carbon dioxide: The critical role of ocean surface water in high latitudes. *The Carbon Cycle and Atmospheric CO: Natural Variations Archean to Present*, *32*, 163–184. https://doi.org/10.1029/GM032p0163

Van Andel, T. H. (1975). Mesozoic/Cenozoic calcite compensation depth and the global distribution of calcareous sediments. *Earth and Planetary Science Letters*, *26*(2), 187–194. https://doi.org/10.1016/0012-821x(75)90086-2

Walker, J. C., Hays, P., & Kasting, J. F. (1981). A negative feedback mechanism for the long-term stabilization of Earth's surface temperature. *Journal of Geophysical Research*, *86*(C10), 9776–9782. https://doi.org/10.1029/jc086ic10p09776

Zeebe, R. E. (2012). LOSCAR: Long-Term ocean-atmosphere-sediment CArbon cycle reservoir model v2.0.4. *Geoscientific Model Development*, *5*(1), 149–166. https://doi.org/10.5194/gmd-5-149-2012

Zeebe, R. E., & Caldeira, K. (2008). Close mass balance of long-term carbon fluxes from ice-core CO_2 and ocean chemistry records. *Nature Geoscience*, *1*(5), 312–315. https://doi.org/10.1038/ngeo185

Zeebe, R. E., & Tyrrell, T. (2019). History of carbonate ion concentration over the last 100 million years II: Revised calculations and new data. *Geochimica et Cosmochimica Acta*, *257*, 373–392. https://doi.org/10.1016/j.gca.2019.02.041

Zeebe, R. E., & Westbroek, P. (2003). A simple model for the $CaCO_3$ saturation state of the ocean: The "Strangelove," the "Neritan," and the "Cretan" Ocean. *Geochemistry, Geophysics, Geosystems*, *4*(12), 163–184. https://doi.org/10.1029/2003gc000538

Zeebe, R. E., & Wolf-Gladrow, D. (2001). *CO2 in seawater: Equilibrium, kinetics, isotopes* (p. 346). Elsevier.

Zhou, X., Rosenthal, Y., Haynes, L., Si, W., Evans, D., Huang, K.-F., et al. (2021). Planktic foraminiferal Na/Ca: A potential proxy for seawater calcium concentration. *Geochimica et Cosmochimica Acta*, *305*, 306–322. https://doi.org/10.1016/j.gca.2021.04.012

Ziveri, P., de Bernardi, B., Baumann, K.-H., Stoll, H. M., & Mortyn, P. G. (2007). Sinking of coccolith carbonate and potential contribution to organic carbon ballasting in the deep ocean. *Deep Sea Research Part II: Topical Studies in Oceanography*, *54*(5–7), 659–675. https://doi.org/10.1016/j.dsr2.2007.01.006

19449224, 2023, 6, Downloaded from https://agupubs.onlinelibrary.wiley.com/doi/10.1029/2022GB007541, Wiley Online Library on [26/05/2023]. See the Terms and Conditions (https://onlinelibrary.wiley.com/terms-and-conditions) on Wiley Online Library for rules of use; OA articles are governed by the applicable Creative Commons License